

Supporting Information

Cucurbituril-protected dual-readout gold nanoclusters for sensitive fentanyl detection in sewage

Kun Yan,^a Lancheng Wang,^a Zhihang Zhu,^a Shiqi Duan,^a Zhendong Hua,^b Peng Xu,^b Hui Xu,^a Chi Hu,^{*a} Youmei Wang,^{*b} and Bin Di^{*a}

^a China National Narcotics Control Commission - China Pharmaceutical University

Joint Laboratory on Key Technologies of Narcotics Control, No. 24 Tongjiaxiang
Road, Nanjing 210009, China.

^b Key Laboratory of Drug Monitoring and Control, Drug Intelligence and Forensic
Center, Ministry of Public Security, Beijing, China.

Corresponding Author:

Chi Hu, E-mail: chihu@cpu.edu.cn;

Youmei Wang, E-mail: youmei_626@163.com;

Bin Di, E-mail: dibin@cpu.edu.cn

Contents

Optimization of macrocyclic host.....	S3
Optimization of Q7 concentration.....	S4
DLS.....	S5
HR-TEM images.....	S6
¹H NMR spectroscopic titration.....	S6
Stoichiometric evaluation.....	S7
Calculation of binding constants <i>K</i>.....	S8
Emission and UV-vis titrations.....	S9
Method comparison.....	S10
References.....	S11

Optimization of macrocyclic host

In order to obtain more excellent sensor for FEN detection, the relative values of fluorescence quantum yield for free FGGC-AuNCs and FGGC-AuNCs assembled with Q_n (n=5-8) were measured according to literature method using rhodamine B as fluorescence standard (quantum yield 0.31, in water).¹ The results were shown in table S1. Obviously, Q7 displayed the optimal ability to brighten FGGC-AuNCs, which was finally used for further assay of FEN.

Table S1 Quantum yield of FGGC-AuNCs with and without added Q_n in aqueous solution

Added Q _n	Yield
-	0.0616 ± 0.003
Q5	0.0613 ± 0.001
Q6	0.0617 ± 0.003
Q7	0.5616 ± 0.023
Q8	0.3965 ± 0.018

Optimization of Q7 concentration

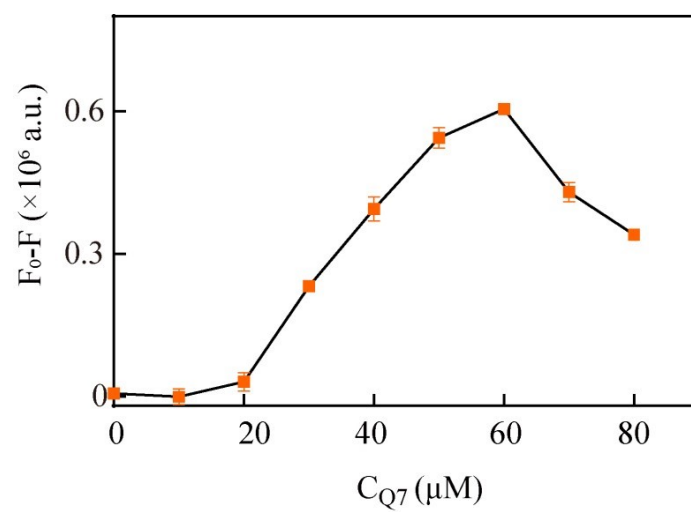


Fig. S1 The effect of FEN ($5 \mu\text{g mL}^{-1}$) on emission spectra of FGGC-AuNCs self-assembled with different concentrations of Q7.

DLS

DLS was used to investigate the hydrodynamic diameter of FGGC-AuNCs, FGGC-AuNCs@Q7 and FGGC-AuNCs@Q7 added with FEN. As shown in Fig. S2, the results of DLS showed the size of 1.8 ± 0.3 nm for FGGC-AuNCs, 1057.2 ± 178.8 nm for FGGC-AuNCs@Q7 and 30.7 ± 3.0 nm for FGGC-AuNCs@Q7 added with FEN. Q7 caused obvious self-assembled aggregation for FGGC-AuNCs. However, the hydrodynamic diameter of FGGC-AuNCs@Q7 was far larger than that measured by HR-TEM, which might be attributed to the nanoscale polymer network under the surface-assembly of Q7 or the dehydration of samples during the TEM preparation. After addition of FEN, the hydrodynamic diameter was reduced and a weak peak for free FGGC-AuNCs was observed, which was also appeared in TEM images (Fig. S3B). These evidences further strengthened that Q7 could cause the aggregation of FGGC-AuNCs and FEN could result in depolymerization of FGGC-AuNCs@Q7 by competitive binding with Q7.

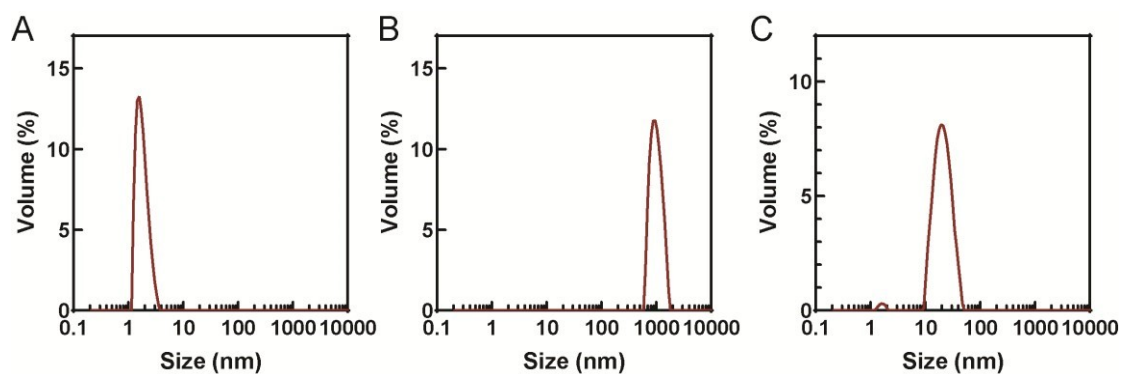


Fig. S2 Hydrodynamic diameter of (A) synthesized FGGC-AuNCs, (B) self-assembled FGGC-AuNCs@Q7 and (C) FGGC-AuNCs@Q7 added with FEN determined by DLS.

HR-TEM images

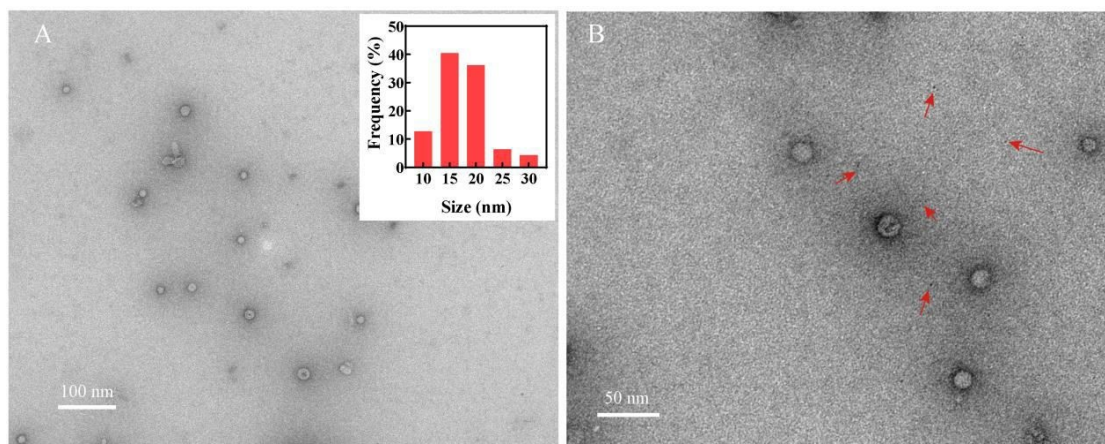


Fig. S3 HR-TEM images of self-assembled FGGC-AuNCs@Q7 added with FEN. Inset: size distribution histograms calculated from images. Free FGGC-AuNCs were marked by red arrows.

^1H NMR spectroscopic titration

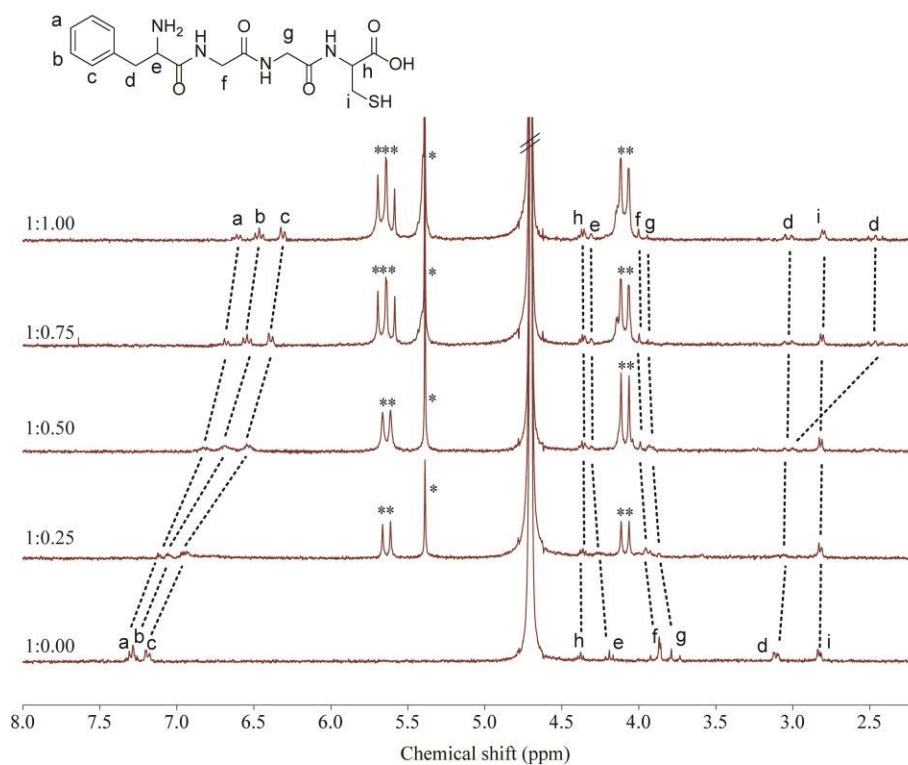


Fig. S4 ^1H NMR titration of Q7 into FGGC (1 mM) in D_2O . Molar ratio of FGGC to

Q7 increases from 1:0.00 to 1:1.00 from bottom to top. Asterisk indicates assignment of Q7 protons.

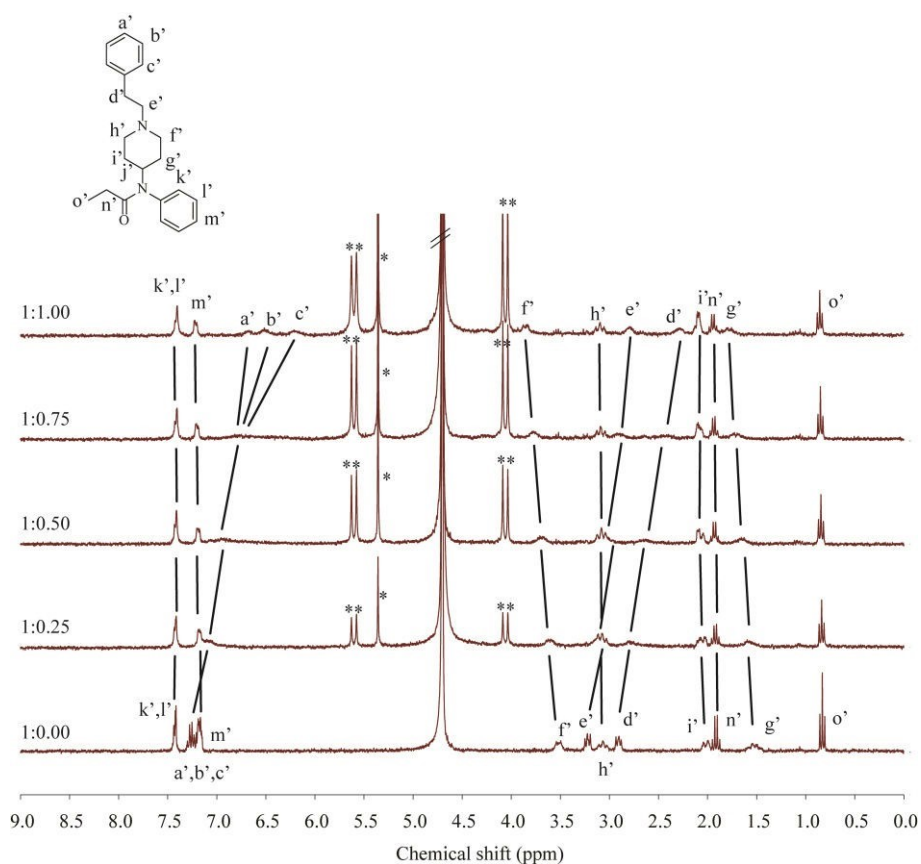


Fig. S5 ^1H NMR titration of Q7 into FEN (1 mM) in D_2O . Molar ratio of FEN to Q7 increases from 1:0.00 to 1:1.00 from bottom to top. Asterisk indicates assignment of Q7 protons.

Stoichiometric evaluation

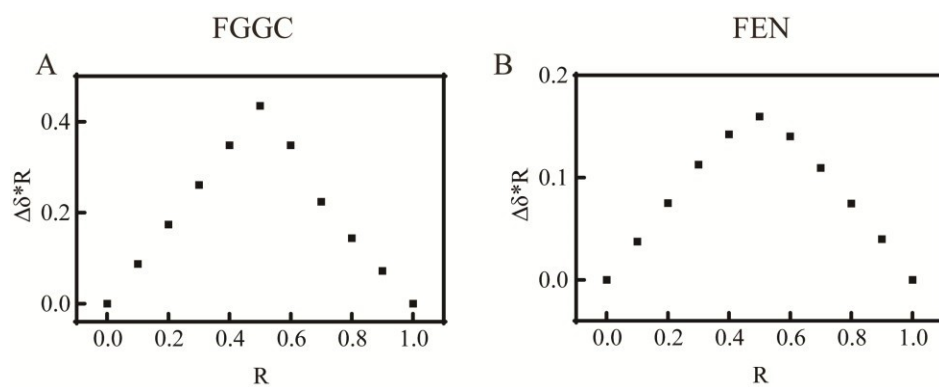


Fig. S6 Job's plots calculated by chemical shifts. R indicates the mole fractions of

guests. A: chemical shifts of proton c of FGGC were monitored; B: chemical shifts of proton f' of FEN were monitored.

Calculation of binding constants K

The values of K were calculated by the Benesi-Hildebrand method.^{2,3} The following equation Eq. 1 was used for the binding stoichiometry of 1:1.

$$\frac{1}{\delta - \delta_0} = \frac{1}{\delta' - \delta_0} + \frac{1}{(\delta' - \delta_0)[Q7]} \quad \text{Eq. 1}$$

where δ is the chemical shift of guest under different concentration of Q7, and δ_0 is the chemical shift of guest in the absence of Q7. K is the binding constant of the complex, which was calculated from the ratio of intercept to the slope. The linear relationship between $1/(\delta - \delta_0)$ and $1/[Q7]$ was shown in Fig. S7.

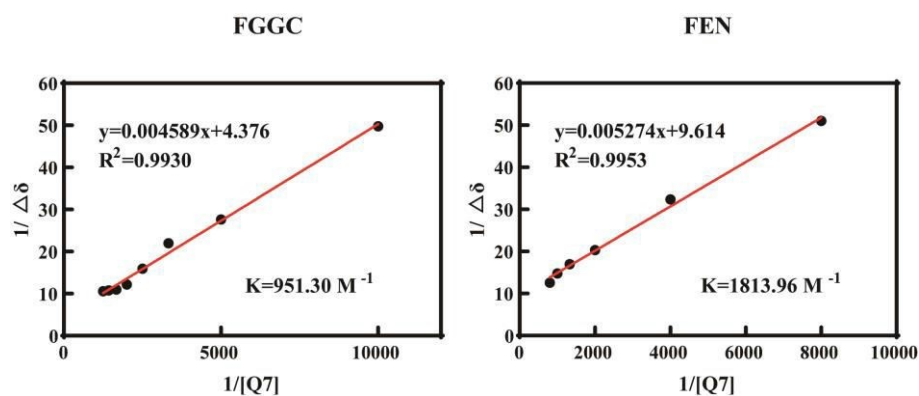


Fig. S7 Benesi-Hildebrand plots of $1/(\delta - \delta_0)$ versus $1/[Q7]$ based on ^1H NMR signal changes.

Emission and UV-vis titrations

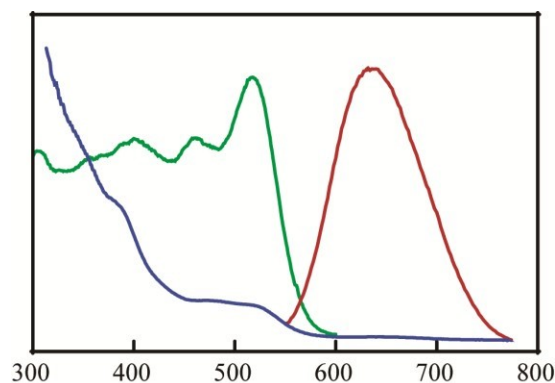


Fig. S8 The absorption spectrum (blue), excitation spectrum (green), and emission spectrum (red) of FGGC@AuNCs in aqueous solutions.

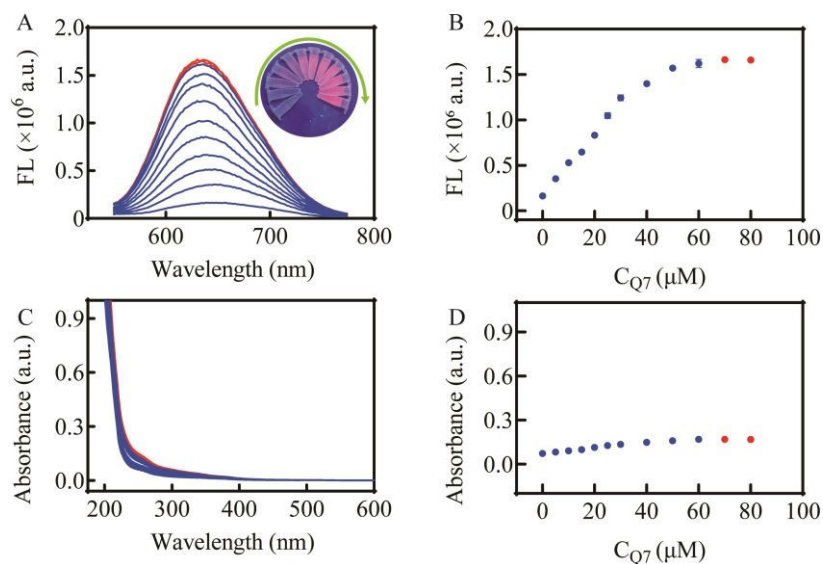


Fig. S9 Emission spectra (A) and normalized fluorescence at 640 nm (B) of FGGC-AuNCs with the increasing concentration of Q7 in aqueous solutions at the excitation wavelength of 515 nm. Inset: eppendorf tubes containing the corresponding solutions under 365 nm light. UV-vis spectra (C) and normalized absorbance at 275 nm (D) of FGGC-AuNCs with the increasing concentration of Q7 in aqueous solutions.

Method comparison

Table S2 Comparison of the present method with previous methods for fentanyl detection

Detection method	Description	Application	Linear range (ng mL ⁻¹)	LOD (ng mL ⁻¹)	Ref.
Electrochemical	Single-walled carbon nanotubes	-	-	3696	4
Immunoassay	Test strips	Urine		100	5
SERS	AgNPs and microfluidic device	Forensic analysis and quantitation		100	6
Colorimetry	SDS/Rose Bengal	Diluted urine and domestic sewage	4020-29915	700	7
Colorimetry	Rose Bengal	Soft beverages	201-20100	100	8
Fluorescence	FGGC-AuCNs@Q7	Diluted urine	9-148000	1	This work

SDS: Sodium dodecyl sulfate

References

1. X. Lv, C. Gao, T. Han, H. Shi and W. Guo, *Chemical Communications*, 2020, **56**, 715-718.
2. X. Cai, R. Kataria and B. C. Gibb, *J. Am. Chem. Soc.*, 2020, **142**, 8291-8298.
3. Y. Jin, W. Sun, H. Lv and S. Tong, *Chirality*, 2020, **32**, 1257-1263.
4. N. Wester, E. Mynttinen, J. Etula, T. Lilius, E. Kalso, B. F. Mikladal, Q. Zhang, H. Jiang, S. Sainio, D. Nordlund, E. I. Kauppinen, T. Laurila and J. Koskinen, *ACS Appl. Nano Mater.*, 2020, **3**, 1203-1212.
5. T. C. Green, J. N. Park, M. Gilbert, M. McKenzie, E. Struth, R. Lucas, W. Clarke and S. G. Sherman, *Int. J. Drug Policy*, 2020, **77**, 102661.
6. A. Haddad, M. A. Comanescu, O. Green, T. A. Kubic and J. R. Lombardi, *Anal. Chem.*, 2018, **90**, 12678-12685.
7. Y. Lin, J. Sun, M. Tang, G. Zhang, L. Yu, X. Zhao, R. Ai, H. Yu, B. Shao and Y. He, *Anal. Chem.*, 2021, **93**, 6544-6550.
8. Y. Lin, J. Sun, X. Xiang, H. Yu, B. Shao and Y. He, *Sens. Actuators B Chem.*, 2022, **354**, 131215.